Fragmentation

E. Villermaux

Université de Provence, IRPHE, Marseille & Institut Universitaire de France, Marseille cedex 13, 13384 France; email: emmanuel.villermaux@irphe.univ-mrs.fr

Annu. Rev. Fluid Mech. 2007. 39:419–46

The *Annual Review of Fluid Mechanics* is online at fluid.annualreviews.org

This article's doi:
10.1146/annurev.fluid.39.050905.110214

0066-4189/07/0115-0419$20.00

Key Words

atomization, breakup, ligaments, capillarity, statistical distribution

Abstract

Fragmentation phenomena are reviewed with a particular emphasis on processes that give rise to drops—in the broad sense, the process of atomization. Various observations are brought together to give a unified picture of the overall transition between a compact macroscopic liquid volume and its subsequent dispersion into stable drops. In liquids, primary instabilities always give birth to more or less corrugated ligaments whose breakup determines the shape of the drop-size distribution in the resulting spray. Examples examined here include fragmentation of jets and liquid sheets, formation of spume by the wind blowing over a liquid surface, bursting phenomena upon an impact, and raindrops.

1. A TIMELESS TOPIC

"Grinding, porphirization, and spraying are, strictly speaking, nothing but preliminary mechanical operations aiming at dividing, separating molecules from bodies, and reducing them in very fine particles."

ANTOINE LAURENT LAVOISIER, *Traté Élémentaire de Chimie*
Librairie Cuchet, Paris, 1789.

The fragmentation of compact macroscopic objects is a typical phenomenon involving complicated microscopic effects, and resulting in nontrivial, and often broad statistics, namely that of the fragment sizes. Very recently, in fact from the time when the need was felt to rationalize empirical practices in ore processing (Georg Bauer 1556), questions about the principles of matter division have been recurrent in science, up to modern developments in nuclear fission (Born 1969). For instance, Lavoisier (1789) devotes chapter IV of his *Elementary Treatise of Chemistry* to different techniques for dividing matter, and the monumental treatise of Coulson & Richardson (1968) has several sections dealing with the many "unit operations" of the chemical industry to fragment, atomize, blend, and mix. The long history of the subject is certainly not a sign of lack of progress, but rather reflects its ever-renewed fields of application.

As for liquid atomization (literally "subdivide down to the atom size"), examples abound, ranging from agricultural sewage, diesel engines, and liquid propellant combustion in the aerospace industry (Bayvel & Orzechowski 1993, Lefebvre 1989, Yang & Anderson 1995), geophysical balances and ocean-atmosphere exchanges (Blanchard 1966, Mason 1971, Seinfeld & Pandis 1998), volcanic eruptions and tephra formation (Alidibirov & Dingwell 1996), sprayed paint and cosmetics, ink-jet printers, microfluidic, and novel devices (Squires & Quake 2005, Stone et al. 2004). For all of these applications, it is desirable to have an a priori knowledge of the liquid dispersion structure, in particular its distribution of droplet sizes as a function of the control parameters, injector size and shape, wind speed, liquid surface tension, etc.

1.1. Problem Statement

The subject matter is probably all contained in **Figure 1**, which shows how a liquid drop, falling in a counter-ascending air current, first deforms, then destabilizes, and finally breaks into disjointed, stable fragments. The process, usually called "bag breakup," exemplifies the three stages shared by all atomization processes:

- A change of topology of the initial object: The big drop flattens to a pancake shape as it decelerates downward.
- The formation of ligaments: The toroidal rim collects most of the initial drop volume.
- A broad distribution of fragment sizes: The rim is highly corrugated and breaks in many small, and some large, drops.

If Δu is the velocity difference between the drop and the air stream in a Galilean frame, the drop will break as soon as the stagnation pressure of order $\rho_g(\Delta u)^2$

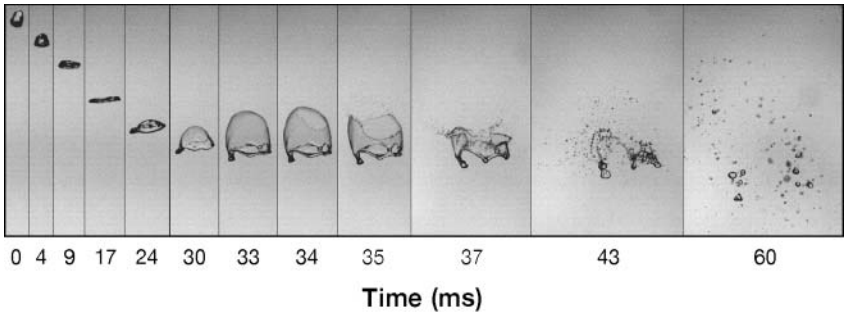

Figure 1

Fragmentation of a 5-mm water drop falling relative to to an ascending stream of air. Times from the first image ($t = 0$) are: $t = 4$, 9, 17, 24, 30, 33, 34, 35, 37, 43, and 60 ms.

overcomes the capillary restoring pressure σ/d_0, where ρ_g, d_0, and σ represent the gas density initial drop size, and σ the liquid surface tension, respectively. This condition indicates that the Weber number

$$We = \frac{\rho_g(\Delta u)^2 d_0}{\sigma} \tag{1.1}$$

should be larger than some number (Hanson et al. 1963, Hinze 1955), with some corrections accounting for possible viscous effects (Chou & Faeth 1998, Pilch & Erdman 1987). In this, as in many atomization processes, there is no typical fragment size. There is an average size, and an obvious upper bound, namely the size of the initial drop. It is even unclear if there should be a lower bound. However, the hierarchy of fragment sizes d follows a regular distribution $p(d)$, with the probability of finding a drop size between d and $d + \mathrm{d}d$, essentially uniformly decreasing in an exponential-like form with d

$$p(d) \sim e^{-d/d_0} \tag{1.2}$$

up to some cutoff parametrized by the drop's initial size d_0 (Alusa & Blanchard 1971, Kombayasi et al. 1964). This review illustrates the characteristics of $p(d)$ and discusses the possible underlying mechanisms.

2. SMART IDEAS

The ubiquity of fragmentation phenomena has prompted a number of interpretations and paradigms. These can be grouped into roughly three distinct classes.

2.1. Sequential Cascades of Breakups

A first class of models was introduced by Kolmogorov (1941), motivated by ore grinding, a process where repeated forcings are sequentially imparted to brittle solid particles; the model has been applied, blindly after a detour in the turbulence community (Monin & Yaglom 1975), to liquid atomization. The overall breakup is visualized as a sequential process where mother drops give rise to daughter drops, which break into smaller drops. The sense of the evolution of the drops assembly is directed toward ever smaller sizes. In this cascade process and many of its variants (see e.g., Gorokhovski & Saveliev 2003, Konno et al. 1983, Martinez-Bazan et al. 1999, Novikov &

Dommermuth 1997), a particle of initial volume v_0 breaks, after n steps of the cascade into a family of drops of volume $v_n = v_0 \prod_{i=0}^{n-1} \alpha_i$, where the α_i are random multipliers smaller than unity so that the logarithm $\ln(v_n/v_0)$ is actually a sum of random variables

$$\ln \frac{v_n}{v_0} = \sum_{i=0}^{n-1} \ln \alpha_i. \tag{2.1}$$

The distribution of the volumes $\mathcal{P}(v)$ is described around its maximum for sufficiently large n and at the precision $1/\sqrt{n}$ in the frame of the Central Limit Theorem (Feller 1971, Kolmogorov 1941) by a lognormal distribution (see, however, Frisch & Sornette 1997)

$$\mathcal{P}\,(x = v/v_0) \to \frac{1}{xS\sqrt{2\pi n}} \exp\left(-\frac{(\ln x - nM)^2}{2nS^2}\right), \tag{2.2}$$

where

$$M = \frac{1}{n}\sum_{i=0}^{n-1} \ln \alpha_i \quad \text{and} \quad S^2 = \frac{1}{n}\sum_{i=0}^{n-1} (\ln \alpha_i)^2 - M^2 \tag{2.3}$$

are the mean and variance of the distribution of the random multipliers α_i, a priori fixed for a given atomization protocol. Defining the size of a drop d by $d_n^3 = v_n$, the drop-size distribution is derived from conservation of probability $p(d) = 3d^2\mathcal{P}(v = d^3)$. The mean $\langle d \rangle$ and variance $\langle d^2 \rangle$ of the size distribution both depend exponentially on n and are such that

$$\frac{\langle d^2 \rangle - \langle d \rangle^2}{\langle d \rangle^2} = e^{nS^2/9} - 1 \tag{2.4}$$

is increasing with the cascade step n. If one anticipates that the cascade will terminate at some generation $n = m$ when the Weber number in Equation 1.1 reaches a critical value written for the current drop size $d = d_m$ (the size of the smallest drops in stirred suspensions are indeed found to obey this rule; see, e.g., Clay 1940, Hinze 1955, Kolmogorov 1949, Shinnar 1961), this scenario suggests that, because the width of the distribution increases relative to the mean as n increases (Equation 2.4), the shape of the distribution will depend on the initial Weber number $We = d_0/d_m$.

2.2. Aggregation Scenarii

In contrast to size reduction is the process of aggregation, which is an ensemble of initially small elementary particles that form clusters of increasing average size as they collide and merge. In that case, the sense of the evolution is directed toward ever larger sizes. The paradigm of this process is Smoluchowski's kinetic aggregation, initially imagined to represent the coagulation of colloidal particles moving by Brownian motion in a closed vessel (von Smoluchowski 1917). If $n(v, t)$ is the number of clusters whose volume is between v and $v + dv$, and $K(v, v')$ is the aggregation frequency per cluster between clusters of volumes v and v', then

$$\partial_t n(v,t) = -n(v,t)\int_0^\infty K(v,v')n(v',t)\,\mathrm{d}v' + \frac{1}{2}\int_0^v K(v',v-v')n(v',t)n(v-v',t)\,\mathrm{d}v' \tag{2.5}$$

is an evolution equation of a convolution type to which additional effects such as liquid evaporation can be added in the form of a Liouville term $-\partial_v\{q(v)n(v,t)\}$ if $q(v)$ is the rate of change of v due to evaporation (Seinfeld & Pandis 1998). The volume distribution of the drops $\mathcal{P}(v,t)$ is equal to $n(v,t)/N(t)$, with $N(t)=\int_0^\infty n(v,t)\,\mathrm{d}v$ the total number of clusters. This framework has been used for modeling the concomitant breakup and coalescence of drops in emulsions (Coulaloglou & Tavlarides 1977), turbulent clouds of drops (Saffman & Turner 1956), gas-liquid dispersions in stirred media (Valentas & Amundson 1966), and breath figures (Derrida et al. 1991) with suitably adapted frequency factors $K(v,v')$. Schumann (1940) and Friedlander & Wang (1966) provide general similarity solutions for various forms of the interaction kernel $K(v,v')$, which all display an exponential tail

$$\mathcal{P}(v,t\to\infty)\overset{v\gtrsim\langle v\rangle}{\longrightarrow}e^{-v/\langle v\rangle}, \tag{2.6}$$

where $\langle v\rangle=\int_0^\infty vn(v,t)\,\mathrm{d}v/N(t)$ is the average volume function of time. The reason is easy to understand. Let us say the aggregation frequency is independent of the volume $K\equiv K(v,v')$ and consider the Laplace transform of $n(v,t)$ as $\tilde{n}(s,t)=\int_0^\infty e^{-sv}n(v,t)\,\mathrm{d}v$. Equation 2.5 is then

$$\partial_t\tilde{n}=-\tilde{n}N+\frac{\tilde{n}^2}{2} \tag{2.7}$$

when $n(v,t)\equiv n(v,t)/N(0)$, $N\equiv N/N(0)$, and $t\equiv tKN(0)$ have been made dimensionless using $N(0)$ as the initial number of clusters. The current total number of clusters $N=\int_0^\infty n(v,t)\,\mathrm{d}v=\tilde{n}(0,t)$ obeys

$$\partial_t N=-\frac{N^2}{2},\quad\text{so that}\quad N=\frac{1}{1+t/2}. \tag{2.8}$$

Looking for a scaling solution to Equation 2.7 of the form

$$\begin{cases} n(v,t)=\dfrac{N}{\langle v\rangle}f(\eta,\tau)\\ \eta=\dfrac{v}{\langle v\rangle}\\ \tau=t, \end{cases} \tag{2.9}$$

having $\tilde{n}(s,t)=N\tilde{f}(s',t)$ with $s'=s\langle v\rangle$ and remembering that

$$\partial_t\tilde{f}=\frac{\partial\tilde{f}}{\partial s'}\frac{\partial s'}{\partial t}+\frac{\partial\tilde{f}}{\partial\tau}\frac{\partial\tau}{\partial t}, \tag{2.10}$$

one is left to find a solution to

$$s'\partial_{s'}\tilde{f}=-\tilde{f}+\tilde{f}^2 \tag{2.11}$$

in the stationary limit $\partial_t\tilde{f}\to 0$. The solution is $\tilde{f}(s',t)=(1+s')^{-1}$, giving

$$f(\eta)=e^{-\eta}\quad\text{that is}\quad n(v,t)=\frac{N}{\langle v\rangle}e^{-v/\langle v\rangle} \tag{2.12}$$

The asymptotic cluster volume distribution is $\mathcal{P}(v)=n(v,t)/N=e^{-v/\langle v\rangle}/\langle v\rangle$ with $N\langle v\rangle=V$, the (conserved) total volume of the aggregates and N given by

Equation 2.8. The exponential is a consequence of the convolution in Equation 2.7, the signature of aggregation phenomena. Lifshitz & Slyozov (1961) considered a solution for the coarsening of an assembly of droplets exchanging solute by diffusion through the continuous phase in which they are embedded, ingredients which are not those of atomization.

2.3. Maximum Entropy Principle and Random Breakups

Another class of approach considers the random splitting of an initial volume in various disjointed elements in one step. There is no sequential evolution, nor any kinetics a priori associated with this break-up scenario. Essentially inherited from the methods developed for the kinetic theory of gases (Mayer & Mayer 1966) and the physics of polymers (Stockmayer 1943; see also Kapur 1989, who work out many different examples, and Englman 1991 for a review), the idea is to visualize a given volume $v_0 = d_0^3$ as a set of $K = (d_0/d_m)^3$ elementary bricks of volume $v_m = d_m^3$, the linear sizes being, for instance, linked by $We = d_0/d_m$, as in Section 2.1, and to compute the most probable distribution of the disjointed clusters incorporating all the bricks (Cohen 1990, 1991). Let us thus consider a drop broken into N disjointed clusters, among which are scattered the K elementary bricks. We call n_k the number of clusters bearing k bricks, the average number of bricks per cluster being $\langle k \rangle = K/N$. There are obviously a number of ways to realize a given partition $\{n_k\}$. The number of microscopic states leading to a given cluster partition $\{n_k\}$ is

$$w(\{n_k\}) = \frac{N!}{\prod_{k=0}^{K} n_k!} \cdot \frac{K!}{\prod_{k=0}^{K} (k!)^{n_k}}, \tag{2.13}$$

together with the conservation laws

$$\sum_{k=0}^{K} n_k = N, \qquad \text{and} \qquad \sum_{k=0}^{K} k n_k = K. \tag{2.14}$$

The structure of the equation for w is as follows: the number of distinguishable arrangements of the $\{n_k\}$ clusters in the total set of N clusters is $N!/\Pi_k n_k!$, whereas any permutation of the k elements in a given cluster leads to the same macroscopic cluster distribution, hence the factor $K!/\prod_k (k!)^{n_k}$. The number of microscopic states $w(\{n_k\})$ has a maximum for a particular partition $\{n_k\}$ found by letting the n_ks vary by an amount δn_k with the constraints $\delta K = \sum_k k \delta n_k = 0$ and $\delta N = \sum_k \delta n_k = 0$. Looking for the maximum of $w(\{n_k\})$ is equivalent to looking for the maximum of its logarithm; writing $\delta \ln w(\{n_k\}) = 0$ leads to

$$\sum_{k=0}^{K} \delta n_k \{-(\ln n_k + \ln k!) + \alpha k + \beta\} = 0, \tag{2.15}$$

where α and β are Lagrange multipliers such that the conservation laws of Equation 2.14 are satisfied. The optimal distribution $\mathcal{P}(k) = n_k/N$ is a Poisson distribution

$$\mathcal{P}(k) = \frac{n_k}{N} = \frac{\langle k \rangle^k}{k!} e^{-\langle k \rangle} \tag{2.16}$$

of parameter $\langle k \rangle$, the average number of bricks per cluster, as would be readily obtained from binomial counting. This is the distribution of the number of objects in a regular partition of space, when the objects are spread at random as sometimes encountered with low inertia particles in turbulent flows (Eaton & Fessler 1994, Lei et al. 2001). The drop-size distribution follows from $p(d) = 3d^2/d_m^3 \mathcal{P}(k = (d/d_m)^3)$.

In the same line of thought, Longuet-Higgins (1992) gives a variant of this approach by asking what the fragment distribution would be when a volume is crushed at random in exactly m pieces. The answer is

$$\mathcal{P}(x) = m(1-x)^{m-1} \tag{2.17}$$

for a linear segment of length unity where x is the fragment length, with average $\langle x \rangle = 1/(1+m)$. This distribution tends toward a pure exponential characteristic of shot noise $\mathcal{P}(x) \simeq me^{-mx}$ (Poisson intervals) for $m \gg 1$. Longuet-Higgins (1992) also provides the corresponding distribution for random breakup of surfaces and volumes. These purely combinatorial descriptions do not account for any interaction between the clusters as they separate and lead to a fragment-size distributions entirely determined by their mean, as does the convolutive aggregation scenario in Section 4.3.1.

Figure 2 compares the above three classes of models with generic, real (see Section 3), statistically converged distributions. Maximum entropy or aggregation scenarii are far from the truth: Nature does not aggregate nor split liquid volumes at random. Minute but significant differences exist between the lognormal fit and real data; additional proof that liquid atomization does not proceed, as opposed to crushing and grinding, from a sequential cascade of breakups is given in Section 4.3.1.

3. LIGAMENTS: THE SINEWS OF ATOMIZATION

Drops come from the rupture of objects in the form of threads or ligaments; the smooth, uniform, long liquid cylinder has become the paradigm of droplet formation. Following the observations of Mariotte (1686) and Savart (1833) that a liquid jet eventually ends in a train of droplets, subsequent studies have explained why the basic smooth state is unstable (Plateau 1873), how quickly the instability develops (Rayleigh 1879), and how the thread finally disrupts into disjoined parcels (Eggers 1997) down to nanometric scales (Bréchignac et al. 2002) even in the presence of Brownian noise (Eggers 2002, Moseler & Landman 2000). As speculated by Lord Rayleigh in "Some Applications of Photography" (Rayleigh 1891), time-resolved still images, and now high-speed movies, have substantiated these threads in many other situations where a jet is not present from the start as the object mediating drop formation (Einsenklam 1964, Fraser et al. 1963, Hinze & Milborn 1950, James et al. 2003, Krzeczkowski 1980, Lane 1951, Pilch & Erdman 1987, Ranger & Nicholls 1969, Villermaux et al. 2004). The polydispersity of drops results from the dynamics of these ligaments, as suggested by the examples below.

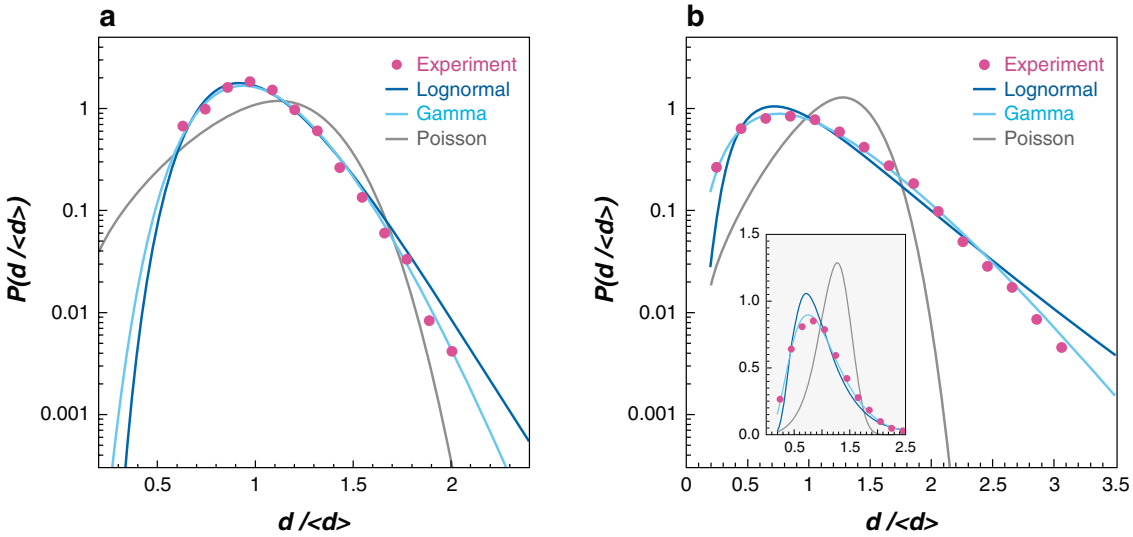

Figure 2

Comparison between experimental records of drop-size distributions in liquid sheet fragmentation (data from Bremond & Villermaux 2006) and different models. The distributions are normalized by their mean and have the same variance $\langle d^2 \rangle$ (Lognormal) and skewness $\langle d^3 \rangle$ (Poisson) as the experimental one. (*a*) Narrow size distribution showing how Lognormal (Section 2.1) and true distributions can be easily confused on a single data set. (*b*) A broader distribution showing how the Lognormal fit overestimates both the distribution around its maximum (*inset*) and its tail. The maximum entropy (Poisson and similarly exponential, Sections 2.3 and 2.2, respectively) distributions have a much-too-sharp falloff (i.e., $\sim \exp\{-(d/\langle d \rangle)^3\}$) at large sizes. The Gamma fit discussed in Section 4.3 has $n = 17$ (*a*) and $n = 4$ (*b*).

3.1. Jets, Sprays, and Spume

The disintegration of a liquid volume by a gas stream is a phenomenon that is involved in many natural and industrial operations. The spray droplets torn off by the wind at the wave crests in the ocean are an obvious example (Andreas et al. 2001, Anguelova & Barber 1999; see also Farago & Chigier 1992 in another context). As **Figure 3** suggests, a shear between the light, fast stream and the slow, dense liquid is at the root of the disintegration process. The change of liquid topology proceeds from a two-stage instability mechanism: First, a shear instability of a Kelvin-Helmholtz type forms axisymmetric waves. It is controlled, as Villermaux (1998a,b) shows, by adapting Rayleigh's (1880b) analysis; the boundary layer of the gas at the interface produces interfacial undulations whose selected wavelength is proportional to $\delta\sqrt{\rho/\rho_g}$, where ρ and ρ_g represent the densities of the liquid and gas, respectively, and δ is the boundary-layer thickness. For a large enough amplitude, these undulations undergo a transverse destabilization, of a Rayleigh-Taylor type, caused by the accelerations imposed on the liquid-gas interface by the passage of the primary undulations. These

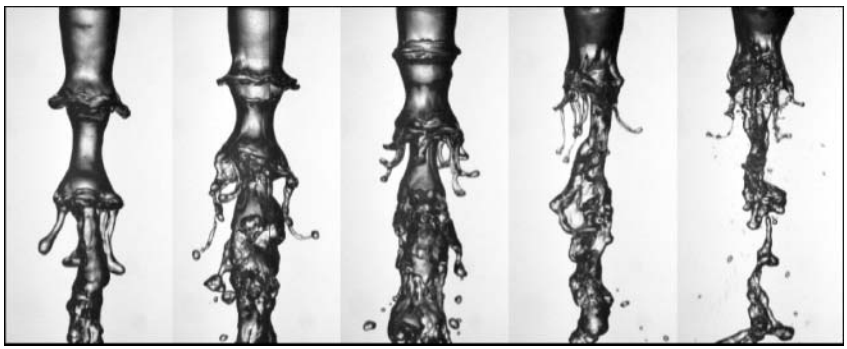

Figure 3

Snapshots of an 8-mm-diameter, slow (0.6 m/s) water jet destabilized by a coaxial fast air stream. Development of the axisymmetric shear instability, digitations at the wave crests, and ligament formation for air velocities increasing from 20 to 60 m/s are shown (Marmottant & Villermaux 2004).

transverse corrugations have a wavelength given by

$$\lambda_\perp/\delta \simeq 3We_\delta^{-1/3}(\rho/\rho_g)^{1/3} \tag{3.1}$$

with $We_\delta = \rho_g u^2\delta/\sigma$, where u is the relative gas velocity. This last instability sets the volume of liquid eventually atomized: The modulation of the crests is further amplified by the air stream–forming ligaments of total volume $d_0^3 \sim \lambda_\perp^3$, ultimately breaking by capillarity (Marmottant & Villermaux 2004).

Ligaments produce final drop sizes larger than their thickness just after they are released from the liquid bulk. This is due to coalescence between the blobs that make up a ligament, an aggregation process that has its counterpart on the shape of the drop-size distribution in the resulting spray $p(d)$, characterized by an exponential falloff. This distribution is the composition of the relatively narrow distribution of the ligament sizes $p_L(d_0)$ and of the distribution of drops sizes coming from the ligament's breakup, which is very well represented by a Gamma distribution (**Figure 4**):

$$p_B(x = d/d_0) = \frac{n^n}{\Gamma(n)}x^{n-1}e^{-nx}. \tag{3.2}$$

The problem is, obviously, Galilean invariant, and the same "stripping" phenomenology occurs when a liquid jet is moving in a still atmosphere, as seen from the early instantaneous pictures of Hoyt & Taylor (1977). The size of the droplets peeled off from the liquid surface decreases with the velocity contrast, given by the liquid velocity (Faith et al. 1995, Wu & Faeth 1995) in that case.

3.2. Sheets

The transition from a compact macroscopic liquid volume to a set of dispersed smaller drops often involves the change of the liquid topology into the shape of a sheet.

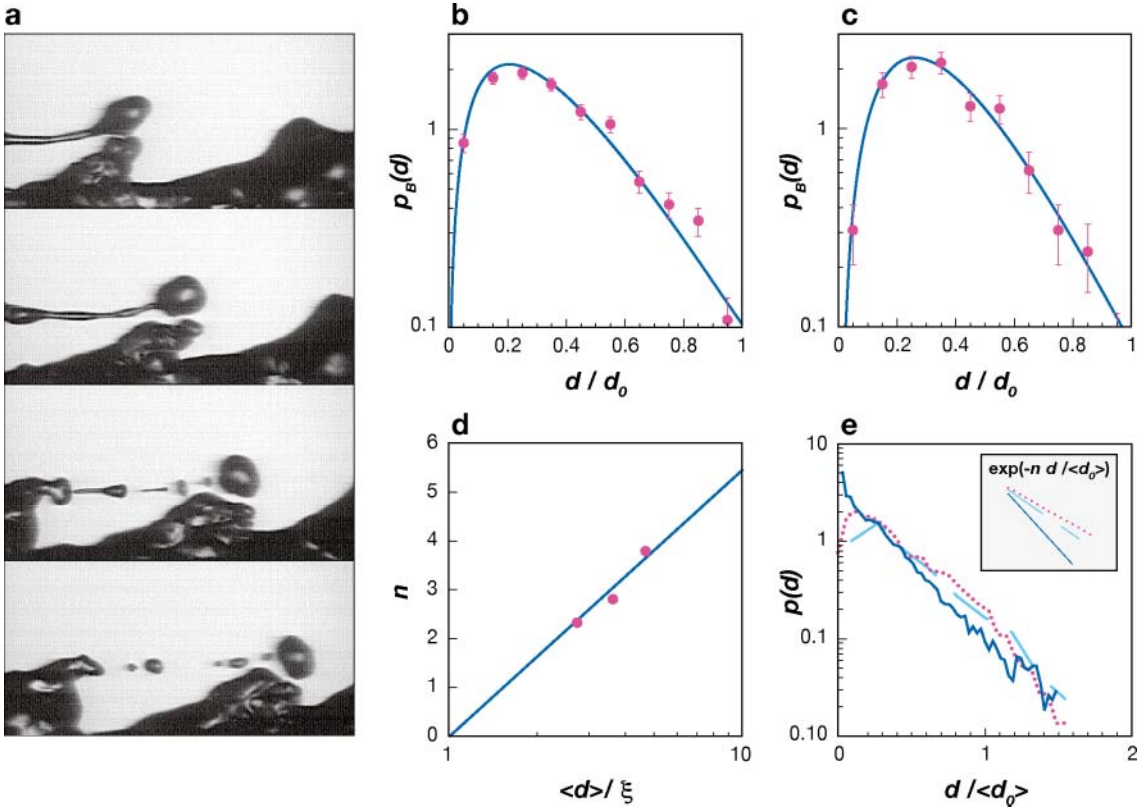

Figure 4

(*a*) Time-resolved series of the elongation and breakup of a ligament in the wind, showing the coalescence between the blobs constitutive of the ligament as it breaks. (*b–e*) Droplet-size distribution after ligament breakup p_B (*d*) for air velocity (*b*) 29 m/s and (*c*) 50 m/s. Lines are fit by Gamma distributions of order *n*. (*d*) Dependence of *n* on the ratio of the average droplet size $\langle d \rangle$ to the ligament thickness at breakup ξ. (*e*) Distribution of droplet sizes in the spray *p*(*d*). The slight increase of the exponential slopes with air velocity (*inset*) reflects the variation of the Gamma orders *n* on $\langle d \rangle / \xi$ (see Section 4.3 and Villermaux et al. 2004).

This transition is sometimes enforced by specific man-made devices, but also occurs spontaneously as a result of various impacts and blowups. An easy way to produce a spray, widely used in the technological context, is to form a liquid sheet by letting a jet impact a solid surface, or a facing jet of like liquid. The sheet disintegrates into drops by the destabilization of its edges. The pioneering works of Savart (1833), and later Taylor (1959a,b) and Huang (1970), essentially focused on the resulting sheet shape and its spatial extension. Depending on the impact Weber number, the radial extension of the sheet is either solely dependent on *We*, or depends both on *We* and on the ratio of the liquid to ambient gas densities $\alpha = \rho_g/\rho$. The transition

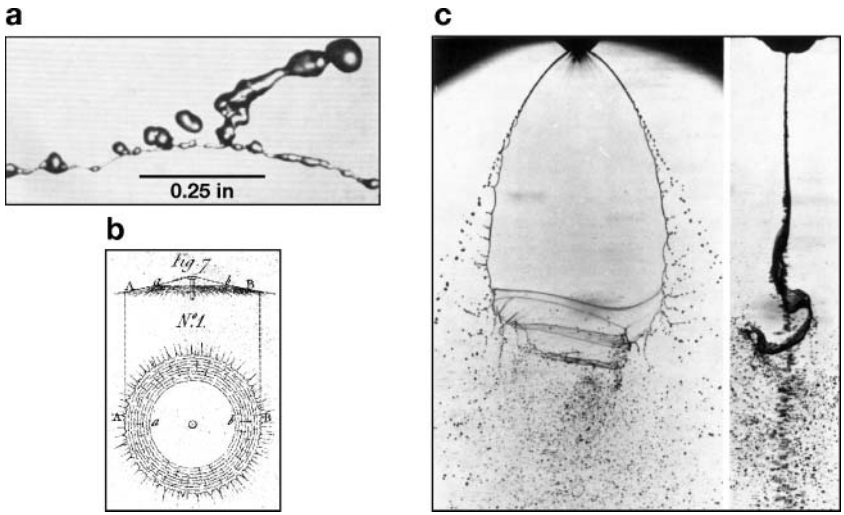

Figure 5

(*a*) A close view of a smooth sheet rim releasing a ligament (Huang 1970). (*b*) Savart's (1833c) drawing of a flapping sheet with undulations and ligaments. (*c*) A liquid sheet from a fan spray nozzle (Crapper et al. 1973).

(Villermaux & Clanet 2002) occurs for

$$We = \mathcal{O}(\alpha^{-1/2}). \tag{3.3}$$

Below this limit the sheet is smooth, and above it sustains a shear, flag-like instability (Hagerty & Shea 1955, Squire 1953, Taylor 1960, York et al. 1953; see also Lin 2003). Aside from interesting conjectures and suggestions (Dombrowski & Johns 1963, Fraser et al. 1962, York et al. 1953), the quantitative study of the drop-formation process was only recently addressed (Bremond & Villermaux 2006, Clanet & Villermaux 2002, Villermaux & Clanet 2002). While drops of the order of the jet diameter are formed from the destabilization of the thick rim bordering the sheet in the smooth regime, the average drop size is a strongly decreasing function of the Weber number in the flapping regime (**Figure 5**). In all cases, the sheet fragments by the destabilization of its rim, which form cusps at the tip of which ligaments are ejected, are a prelude to the drop formation. These ligaments were actually already present in Savart's (1833) early drawings and have been observed by Mansour & Chigier (1990) and more recently by Park et al. (2004) with air-blasted liquid sheets. They also are present from the numerical simulations by Lozano et al. (1998) and Kim & Sirignano (2000) when a spanwise perturbation is initially added to the flow.

In the oblique collision of two identical jets (**Figure 6**), the liquid expands radially forming a sheet in the form of a bay leaf bounded by a thicker rim, but the ligament production phenomenology persists (Anderson et al. 1995, Bremond & Villermaux 2006, Bush & Hasha 2004, Crapper et al. 1973, Dombrowski & Hooper 1963, Dombrowski & Neale 1974, Heidmann et al. 1957, Ryan et al. 1995). This is a particularly interesting configuration because the distribution of the drop sizes can be manipulated at will by varying the impacting angle and Weber number. The volume d_0^3 of massive regions centrifuged along the rim is both insensitive to the external

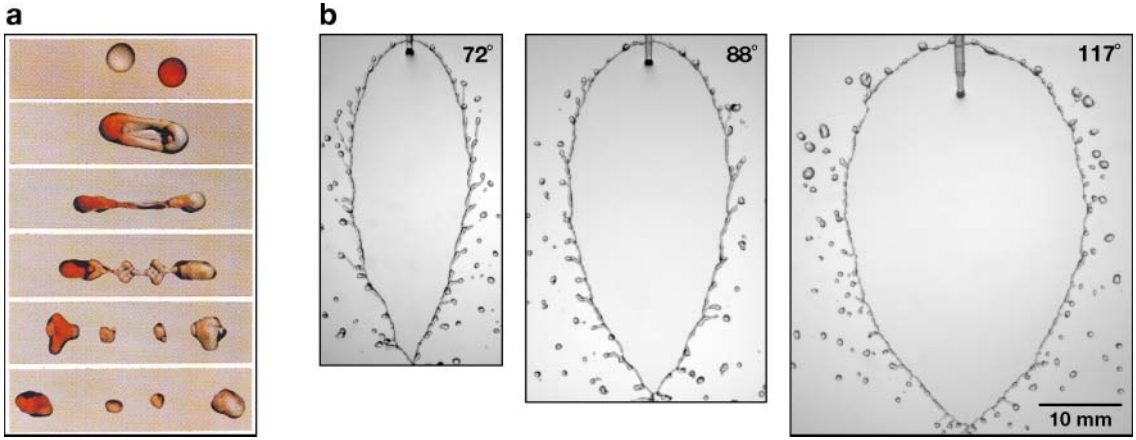

Figure 6

(*a*) Binary collision of drops, stretching, and fragmentation. $We = 83$ based on the relative velocity between the drops (Ashgriz & Poo 1991). (*b*) Water sheet fragmentation for three collision angles. The jet velocity is equal to 4 m/s and the jet diameter is 1.05 mm. Elongation of ligaments is clearly enhanced when the collision angle is decreased (Bremond & Villermaux 2006).

parameters and weakly distributed (**Figure 7**). It elongates and stretches in the form of ligaments, with their feet attached to the rim. The transient development of the capillary instability at the early stages of a ligament elongation sets its section corrugations at the moment it detaches. Corrugations are more pronounced when stretching is weak, resulting in broader size distributions. If the stretch is strong, ligaments are smoother, which results in a narrower distribution. Size distributions pertain to the Gamma family of Equation 3.1 and are parametrized by the single-quantity γ, the rate of stretch in the rim normalized by a capillary timescale, which is a function of both the Weber number and collision angle (**Figure 7**).

3.3. Impacts, Collisions, and Shocks

The change of topology inducing the formation of filamentary structures, which is mandatory for subsequent breakup in drops, is often the result of an impact, either with a solid surface or with a directed source of momentum. An obvious manifestation following the splash of a drop on a solid surface or on a thin fluid layer of the same fluid is the formation of fingers—ligaments emerging from the celebrated Worthington-Edgerton crown (Worthington 1908)—eventually breaking into drops (see Thoroddsen et al. 2006 for fluids of different nature). Most of the attention has been devoted to describing the kinematics of the drop spreading as it flattens on the surface, its maximal extension, and the number of crown fingers (Yarin 2006). However, data on fragmentation following drop collision or impact, a nevertheless salient facet of the phenomenon potentially crucial to understand, if not the universe, at least the structure of the solar system (Stern et al. 2006), are scarce. Ashgriz & Poo (1991)

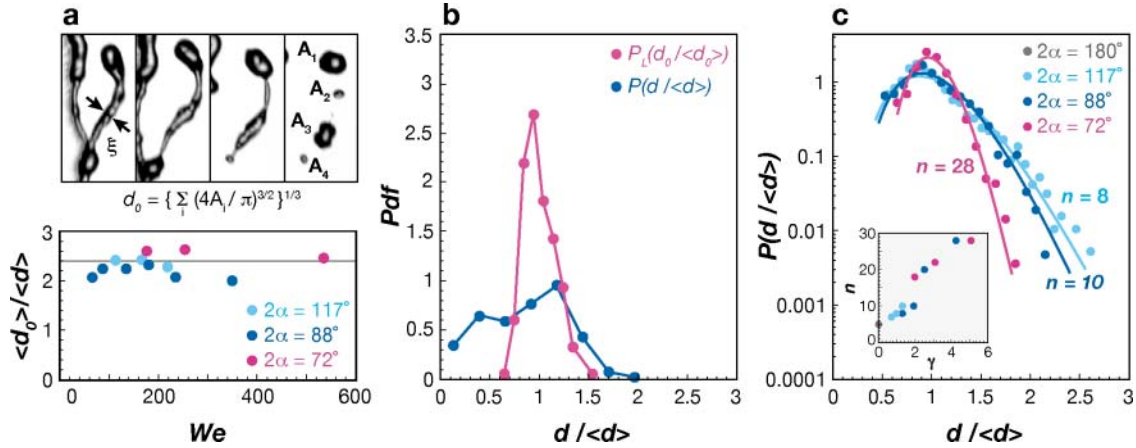

Figure 7

(*a*) The definition of the equivalent sphere diameter of a ligament d_0 and its value normalized by the average drop size for several injection conditions. Typically, $\langle d_0\rangle/\langle d\rangle \approx 2.5$. (*b*) Distributions p_L (d_0) and p_B (d) show that d_0 is less distributed than d. (*c*) Probability density functions of the drop size normalized by the mean drop size $d/\langle d\rangle$ for a fixed impacting velocity $u_j = 3.5$ m/s and three collision angles. The fitted curves are Gamma distributions with parameter n, as indicated in each case and reported in the inset vs dimensionless stretch γ (Bremond & Villermaux 2006).

and Qian & Law (1997) quantified the conditions for coalescence or satellite formation in the binary collisions of drops, and Stow & Stainer (1977) measured the number of fragments of a water drop colliding with a solid surface and their distribution (see also L. Xu, L. Barcos, and S. Nagel 2006, submitted). A liquid film impacted by a shock wave disintegrates via a web of ligaments (Bremond & Villermaux 2005), with patterns resembling those obtained from the spinodal decomposition of liquid films on solid substrates (Elbaum & Lipson 1994, Reiter 1992), but not much is known about the resulting drop-size distribution.

3.4. Rain

Rain has been more thoroughly studied. Bentley (1904), an autodidact farmer of Vermont, captured the very nature of rain using ingenious experiments. He notes, "Perhaps the most remarkable fact, early brought to our notice, was the astonishing difference in the dimensions of the individual drops, both in the same and different rainfalls," singling out that the feature to understand is the distributed character of the drops. At the same time, Lenard (1904), a professor in Heidelberg and a future Nobel Prize winner, was contemplating drops shapes and terminal velocity. Subsequent measurements by Laws & Parsons (1943) and Marshall & Palmer (1948) established the exponential shape of the distribution and related its steepness to the intensity of rainfall: Drops sizes are more broadly distributed in heavy storms than in fine mists, a trend already visible from Bentley's records (**Figure 8**). Existing

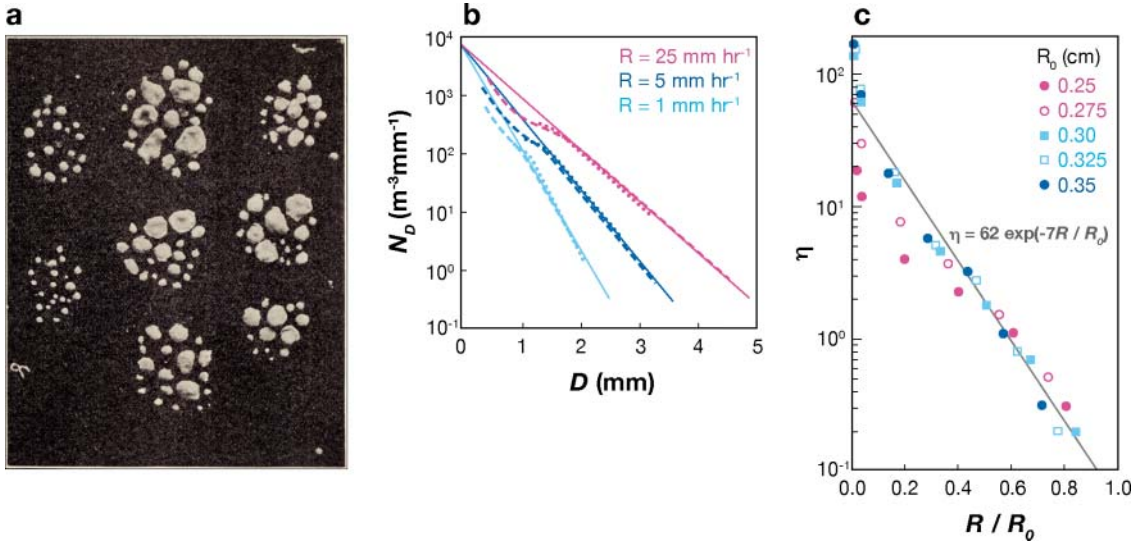

Figure 8

(*a*) Raindrop specimens captured by Bentley (1904) by allowing the drops to fall into a one-inch-deep layer of fine uncompacted flour. (*b*) Drop-size distributions for three different rainfall rates (Marshall & Palmer 1948). (*c*) Cumulative drop-size distribution $\eta = \int_R^\infty p(R, R_0)\mathrm{d}R$ resulting from the breakup of a drop with initial radius R_0 falling in air (Srivastava 1971).

interpretations of these facts pertain to the aggregation scenario recalled in Section 2.2, as well as condensation of ambient water vapor and possibly evaporation of drops (Falkovich et al. 2002, Low & List 1982, Mason 1971, Seinfeld & Pandis 1998), emphasizing the (presumed) role of coalescence of the drops in the falling rain. However, Srivastava (1971) mentions that spontaneous drop breakup could also be incorporated in the global balance describing drop-size populations and, using Kombayasi et al.'s (1964) measurements, arguments to interpret Marshall-Palmer's law on this basis. The polydispersity of raindrops might be due to the multiplicity of fragments from isolated drops breakups (to this respect, comparing **Figures 1** and **8**, the idea is at least tempting), with no appreciable interaction between the drops themselves.

4. LIGAMENT DYNAMICS

At the core of the droplet-formation mechanism, ligaments are produced if certain conditions are fulfilled, and their later evolution obeys general rules.

4.1. A Toy Model to Understand Timescales

A ligament is a more or less columnar object attached by its foot to the liquid bulk from which it has been stripped. When a capillary tube whose end of diameter D

dips into a liquid is rapidly withdrawn from a free surface, it may entrain a ligament (**Figure 9**) at a condition easy to understand by a simple caricature whose interest is to exhibit limit behaviors and timescales: Suppose that the tube elevation H above the surface increases at a constant rate β and that the column length L between the end menisci is proportional to H so that $L = D\exp(\beta t)$ if D is the initial elevation. The liquid can flow out of the column through the attached end whose surface is $S \simeq \pi\xi^2/4$ with a velocity $u = 2\sqrt{\sigma/\rho\xi}$, as indicated by Bernoulli's equation applied between the median region of the column of diameter ξ with capillary pressure $2\sigma/\xi$ and the exit flat surface at zero pressure. With $V = \pi L\xi^2/4$ the column volume, continuity $\mathrm{d}V/\mathrm{d}t = -uS$, is

$$\frac{\mathrm{d}(\xi^2 L)}{\mathrm{d}t} = -2\sqrt{\frac{\sigma\xi^3}{\rho}}, \tag{4.1}$$

which is solved in

$$\frac{\xi}{D} = e^{-\beta t/2}\left\{1 - \frac{2}{3\beta t_D}\left(1 - e^{-3\beta t/4}\right)\right\}^2 \quad \text{with} \quad t_D = \sqrt{\frac{\rho D^3}{\sigma}}. \tag{4.2}$$

For weak stretching ($\beta t_D \ll 1$), the ligament empties completely in a finite time given by the capillary time t_D based on its initial size: $\xi/D = (1 - t/2t_D)^2$. The (unphysical) exponent 2 is a geometrical artifact due to the fixed external length L. The exponent could be 1/3, 2/5, 1/2, 2/3, or 1 depending on the choices dictated by other constraints (Burton et al. 2005, Chen & Steen 1997, Eggers 1997, Gordillo et al. 2005, Marmottant & Villermaux 2004b). Large stretching ($\beta t_D \gg 1$) prevents capillary contraction and the ligament thins at constant volume: $\xi/D \sim \exp(-\beta t/2)$. Note that this caricature is far from true as the ligament shape is itself a solution of the elongation function $H(t)$; the preserved cylindrical shape (with uniform β along the ligament) is only compatible with an elongation linear in time (Frankel & Weihs 1985). Indeed, the column eventually pinches off from its ends and, since it is no longer stretched, fragments into drops (**Figure 9**).

4.2. Linear Rearrangements

Stretching prevents the ligament from emptying and as a corollary damps its destabilization. The early rearrangement dynamics of the fluid particles along a ligament is well described in the slender-slope approximation (Weber 1931). Its radius $r(z, t)$, taken uniformly equal to ξ, is initially ruled by a linear evolution

$$\partial_t^2 r + 2\beta\partial_t r + \frac{3}{4}\beta^2 r - \frac{1}{2t_\xi^2}\left(-\xi^2\partial_z^2 r - \xi^4\partial_z^4 r\right) = 0 \quad \text{with} \quad t_\xi = \sqrt{\frac{\rho\xi^3}{\sigma}}, \tag{4.3}$$

to which an additional term $-3\nu\left(\partial^3_{zzt} r + (\beta/2)\partial_z^2 r\right)$ discovered by Trouton (1906) accounts for viscous slowing that can be added, as well as other corrections that incorporate the possible viscoelastic rheology of the fluid (Oliveira & McKinley 2005), thereby giving the dynamics of the capillary waves (unstable when βt_ξ is weak) along the ligament (Bremond & Villermaux 2006). Note that this solution describes most of the breakup period, the time lapse of the (fundamentally nonlinear)

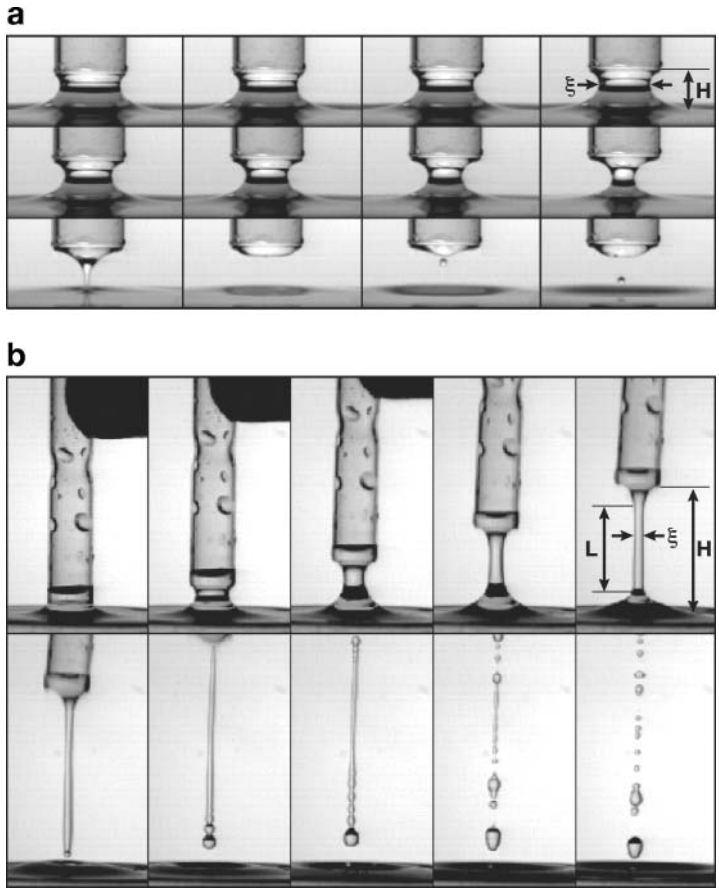

Figure 9

Condition for ligament formation from the withdrawal of a capillary tube (diameter $D = 7$ mm) whose end dips into water (Marmottant & Villermaux 2004b). (*a*) Ligament contraction with a slow tube elevation velocity (time intervals $\Delta t = 10.7$ ms). (*b*) Fast elongation and ligament formation ($\Delta t = 4.5$ ms).

pinching period close to the droplet separation being of order 10^{-3} of the overall breakup period t_ξ (Chen & Steen 1997, Eggers 1997). Most of the time is spent moving the fluid particles apart around the initial ligament shape. Phenomena in the vicinity of the ultimate separation of the particles are comparatively much more rapid.

4.3. Overlapping Random Waves

The statistics of heights of a large number of overlapping waves with random amplitude and phase were first examined by Rayleigh (1880b) and since then the "Rayleigh distribution" has been popular in optics, acoustics, and oceanography (Massel 1996, Roberts & Spanos 1999). Villermaux et al. (2004) proposed another idealization: When two liquid blobs of different sizes d_1 and d_2 (with, say, $d_1 < d_2$) are connected to each other, they aggregate due to the capillary pressure difference $\propto \sigma(1/d_1 - 1/d_2)$. The time it takes for coalescence to be completed is of order $\sqrt{\rho d_1^3/\sigma}$, which is also the time it takes for the neck connecting the two blobs to destabilize and break

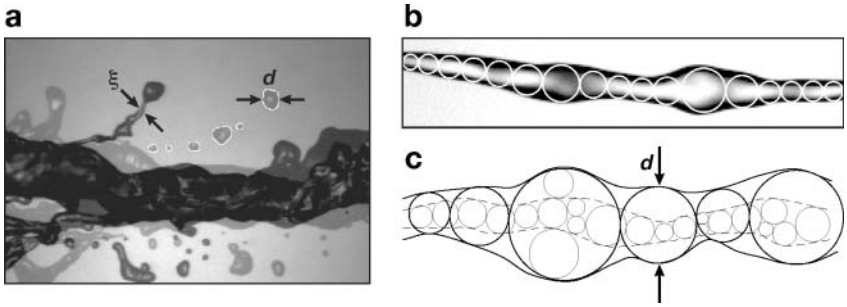

Figure 10

(*a*) Double-flash exposure of a ligament torn off by the wind (Section 3.1) just before and after breakup. (*b*) An isolated ligament covered with blobs of various sizes d matching its local thickness and (*c*) sketch of the layer interaction scheme.

(Section 4.1), which results in a nice "coalescence cascade" (Thoroddsen & Takehara (2000). For this same reason, the blobs constitutive of a ligament tend, as they detach, to coalesce, thereby forming bigger and bigger blobs (see also observations by Oliveira & McKinley 2005). If $n(d,t)d$ is the number of blobs constitutive of a ligament whose size is within d and $d + \mathrm{d}d$ at time t (**Figure 10**), the total number of blobs is $N(t) = \int n(d,t)\,\mathrm{d}d$. Conjecturing that the sizes of the blobs result from a random overlap of independent layers whose widths are set by the mean free path of fluid particles' radial motions across the ligament, the evolution equation for $n(d,t)$ follows lines similar to those recalled in Section 2.2 as

$$\partial_t n(d,t) = -n(d,t)N(t)^{\zeta-1} + \frac{1}{3\zeta-2} n(d,t)^{\otimes\zeta}, \quad \text{with} \quad \zeta = 1 + \frac{1}{n}, \tag{4.4}$$

where $\otimes$ denotes the convolution operation on the linear sizes d. Time t is counted from the moment when the ligament detaches from the liquid bulk and is made nondimensional by $t_\xi = \sqrt{\rho\xi^3/\sigma}$, the capillary time based on the initial average blob size $\xi = \int dn(d,0)\,\mathrm{d}d/N(0)$. Equation 4.4 conserves the net ligament volume $V = \int d^3 n(d,t)\,\mathrm{d}d \equiv d_0^3$. The interaction parameter ζ is determined from the initial distribution of blobs along the ligament by $\zeta = \langle d^2\rangle_0/\xi^2$ with $\langle d^2\rangle_0 = \int d^2 n(d,0)\,\mathrm{d}d/N(0)$. A uniform thread of constant thickness (made of many thin layers) has $\zeta = 1$, and a corrugated ligament (made of a few independent layers) is such that $\zeta > 1$. The asymptotic solution of Equation 4.4 for $p_B = n(d,t)/N(t)$ is a Gamma distribution of order $n = 1/(\zeta-1)$, a convolution of n exponentials arising, as recalled in Section 2.2, from the aggregative construction of $n(d,t)$, providing

$$p_B(x = d/\langle d\rangle) = \frac{n^n}{\Gamma(n)} x^{n-1} e^{-nx}, \tag{4.5}$$

where $\langle d\rangle = \int dn(d,t)\,\mathrm{d}d/N(t)$ is the current average blob diameter. The Gamma shapes fit the experimental distributions of the blob sizes before breakup (**Figure 11**) and the drop sizes after ligament breakup, as substantiated in this review. For an initially corrugated ligament, coalescence between the blobs tends to restore the

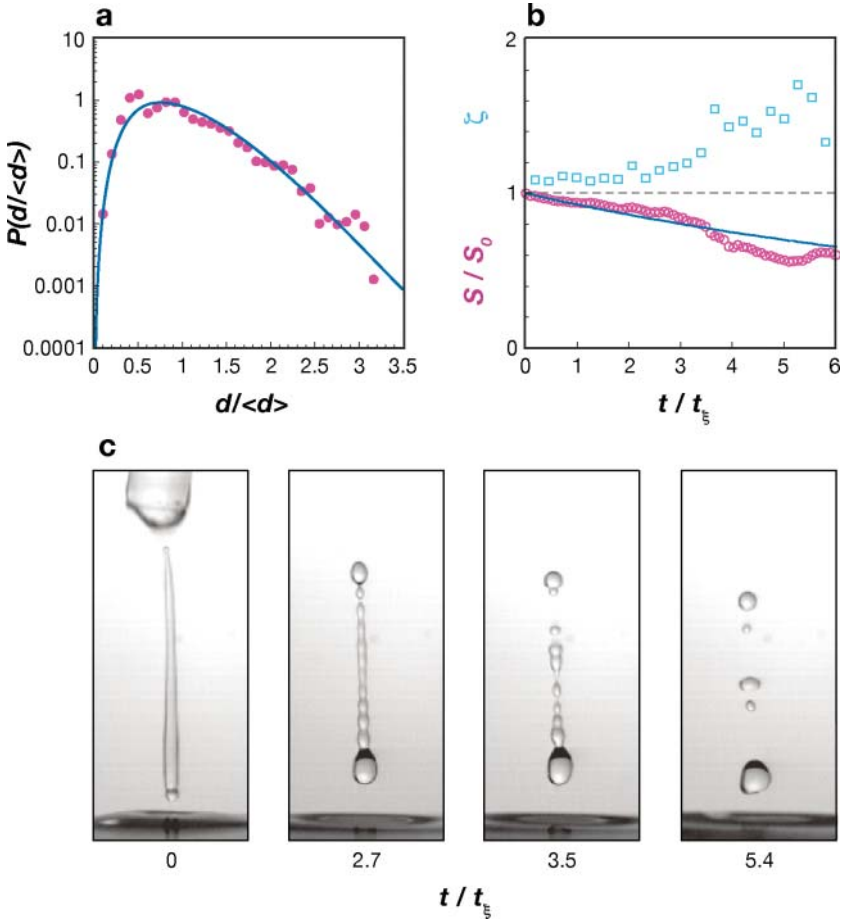

Figure 11

(*a*) Blob-size distribution of the ligament in **Figure 10** just prior to its breakup fitted by a Gamma distribution of order $n = 4.5$. (*b*) Evolution of the roughness ξ of the ligament (*squares*) and of the surface $S/S(t=0)$ (*circles*) as a function of the time in units of the capillary time t_ξ. The continuous line is the prediction for $S(t)$ based on Equation 4.4. (*c*) Corresponding ligament.

average diameter $\langle d\rangle$ from ξ to d_0. This is made at the expense of a reduction of the blob's number, decreasing in time as $N(t)/N(0) = \{1 + N(0)^{1/n}t/n(1+n/3)\}^{-n}$; concomittantly, the average diameter increases like $\langle d\rangle/\xi \sim N(t)^{-1/3}$, and the net projected ligament surface $S(t) = N(t)\int d^2\, p(d,t)\,\mathrm{d}d$ goes like $N^{1/3}$ (**Figure 11**).

4.3.1. Average drop size vs distribution width. The dependence of the resulting average droplet sizes $\langle d\rangle$ on n presents two distinguished limits: For large n, that is, for smooth and uniform ligaments giving rise to a narrow size distribution (width $\sim 1/\sqrt{n}$) centered around ξ, one has

$$\ln\frac{\langle d\rangle}{\xi} \simeq \frac{1}{n}, \tag{4.6}$$

which are drops sizes proportional to the initially smooth thread diameter, as familiar from Rayleigh (1879). For small n, representative of corrugated ligaments,

$$\ln\frac{\langle d\rangle}{\xi} \simeq \ln\left(N(0)^{1/3}\right) - \frac{1}{3}n\ln(n), \tag{4.7}$$

giving an average drop size $\langle d \rangle \approx \xi N(0)^{1/3} = V^{1/3} = d_0$ of the order of the whole ligament volume-equivalent sphere diameter. These barely stretched ligaments break into essentially one big drop plus a few smaller ones and produce the broadest size distributions compared with those encountered in Section 3.1 with wind drops. Equation 4.7 predicts that thinner, but still corrugated, ligaments formed by faster winds, or when the capillary breakup slows down due to an increased liquid viscosity (Mabile et al. 2003, Tucker & Moldenaers 2002) so that the ligament is stretched longer (Bremond & Villermaux 2006), produce not only finer drops, but also a narrower distribution (**Figures 4** and **7**). This trend is opposite to the sequential-cascade mechanism for which the width of the distribution is increasing with cascade step while drop sizes are decreasing (Section 2.1 and Equation 2.4).

When the diameter d_0 is distributed among the ligament's population like $p_L(d_0)$, the size distribution in the spray is $p(d) = \int p_L(d_0) p_B(d/d_0)\, \mathrm{d}d_0$. Generically, $p_B(d/d_0)$ is narrower than $p_L(d_0)$ (**Figure 7**). The composition operation stretches the large excursion wing of $p_B(d/d_0)$ over nearly the whole range of sizes d and the distribution in the spray (**Figure 4**) coincides with an exponential falloff

$$p(d) \sim \exp(-nd/\langle d_0 \rangle) \tag{4.8}$$

whose steepness depends on the average ligament volume through $\langle d_0 \rangle$, which also sets the average drop size in the spray, independent of the Weber number (Simmons 1977a,b)—another fact contrary to the direct-cascade scenario (Sections 1.1 and 2.1). The exponential shape of the spray's size distributions originates from the large excursion tail of Gamma distributions that arise from ligament dynamics, the crucial step of atomization.

5. RELATED SUBJECTS AND FUTURE DIRECTIONS

Two hundred years after the seminal contributions of Laplace and Young (see the perspective given in Pomeau & Villermaux 2006), fragmentation remains an exciting issue in capillary-driven phenomena. Given the diversity of its applications, a number of facets of the subject have not been alluded to in this review, including:

- Scalar mixing: The concentration distribution P of a dye being mixed in a randomly stirred flow obeys a construction rule identical to that building $p_B(d)$ in Section 4.3. The structure $\partial_t P = -P + P^{\otimes 1+1/n}$ giving rise to Gamma distributions is also the one encountered in this context (Villermaux & Duplat 2003) because of the linear character of the Fourier equation describing concentration evolutions and random stirring. Sultan & Boudaoud (2006) made a similarly unexpected and striking analogy regarding the statistics of straight segment lengths in compact crumpled sheets of paper (**Figure 12**).
- Supercritical atomization: At the crossroads between scalar mixing and atomization are the phenomena occurring (and ceasing to occur!) in the immediate proximity of the critical point in the neighborhood of the liquid-vapor transition. There, surface tension and molecular diffusivity vanish. These thermodynamic conditions are sometimes encountered in hydrogen/oxygen rocket

Figure 12

(*a*) A two-dimensional slice of a three-dimensional field of scalar randomly stirred, exhibiting the structure of adjacent sheets coalescing by diffusion. (*b*) A cut through a compactly crumpled sheet of paper. Courtesy of Etienne Couturier.

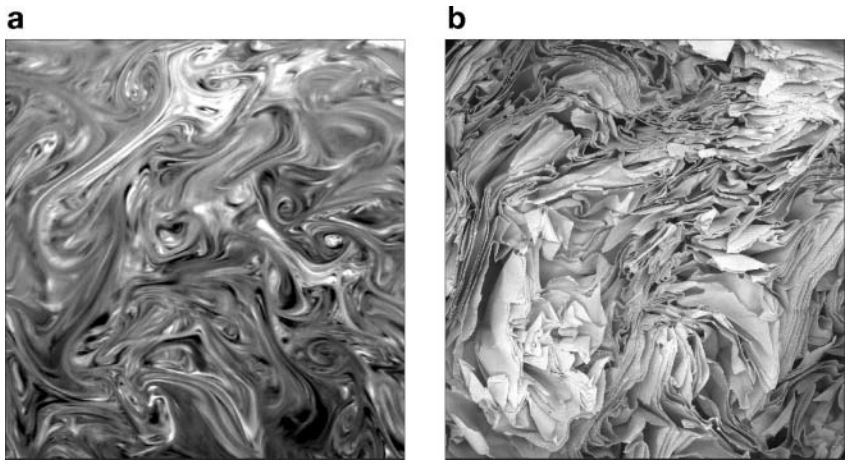

engines (Mayer & Tamura 1996), or realized on purpose to make micronized particles in the pharmaceutical context (Della Porta et al. 2005).

- Bubbles: The examples discussed here were all about liquid drops forming in an evanescent environment. There is no reason to think that the same phenomenology and ideas would not apply to the opposite situation of bubbles forming in a continuous liquid phase: The fundamental instability, that of a hollow ligament in a liquid, is of the same nature as that of a liquid ligament in a vacuum (Chandrasekhar 1961). Bubbles entrained at the sea surface by breaking waves have size distributions that are likely Gamma distributions (Loewen et al. 1996, Wu 1981).
- Effervescent atomization: A fascinating problem and very efficient atomizing process (Sovani et al. 2000) is the explosion of cavities in a liquid volume (expanded microbubbles injected in situ, dissolved gazes, etc.). The two-dimensional version of it, a film bursting by hole nucleation (**Figure 13**), suggests that interesting geometrical ingredients probably influence final drop-size distributions.

Future directions in fragmentation research may concern fundamental issues as well as extensions to other areas, including:

- Ligament dynamics and energetic balances: The idealization of coarsening dynamics in a ligament is, despite its successes, highly conjectural, and it is necessary to make a deeper connection with detailed fluid mechanics. This would, in particular, clarify the partition, while drops separate, between surface energy creation (which represents about 10% of the initial available energy; see Clanet & Villermaux 2002), remnant kinetic energy of the drops (weak in general), and viscous dissipation (therefore, huge)—a question for which we have no ab initio principle (see also Qian & Law 1997).
- Foams: Adjacent cells in a foam have generically different internal pressures, and exchange the embedded gas phase through their separatrix with their neighbors,

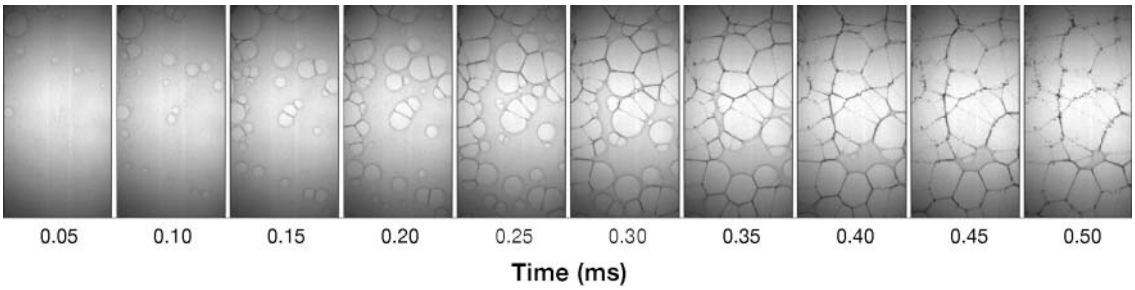

Figure 13

Bursting of a soap film accelerated by the impact of a shock wave. The initially connex film nucleates holes that grow to form a web of ligaments breaking into droplets. Time goes from left to right with time step $\Delta t = 0.05$ ms. Incoming wave Mach number is $M = 1.07$ (Bremond & Villermaux 2005).

resulting in a rate of change of their area determined exactly (in two dimensions) from their number of sides (von Neumann 1952). It will be interesting to see if an interaction rule of a random aggregation type could produce cell area distributions along the paradigm discussed in Section 4.3, an option that has not, surprisingly, been considered.

- Solid fragmentation: Research on solid and liquid fragmentation has often been concomitant, and sometimes conducted by the same experimentalists (Heywood 1933, Rosin & Rammler 1933). Are there common principles? Fragmentation of brittle solids is a world that has developed its own methods, sometimes close to those exposed in Section 2 (Grady & Kip 1985, Mott 1947), and recently inspired by those of critical phenomena (Fisher 1963) in search of universal power laws (Oddershede et al. 1993, Wittel et al. 2004), a description also popular for nuclear fission. However, Gladden et al. (2005) have shown that in dynamical impact of rods, subsets of the fragment sizes could be interpreted by standard linear elasticity. Will the entire distribution be understood along these lines?

ACKNOWLEDGMENTS

Devising the sense hidden behind the apparently confusing phenomenology of fragmentation phenomena is an equally enthusiastic and exhausting task. I am grateful to two of my PhD students, N. Bremond and Ph. Marmottant, for having accepted to follow (and sometimes precede!) me in this difficult enterprise. I am particularly indebted to my colleague Jérome Duplat and his taste for free and deep thinking. Over the years, this work has been supported by the Société Europénne de Propulsion (SEP), the Centre National d'Études Spatiales (CNES), and the Centre National de la Recherche Scientifique (CNRS).

LITERATURE CITED

Alidibirov M, Dingwell DB. 1996. Magma fragmentation by rapid decompression. *Nature* 380:146–48

Alusa A, Blanchard D. 1971. Drop size distribution produced by the breakup of large drops under turbulence. *J. Rech. Atmos.* 7(1):1–9

Anderson WE, Ryan HM, Santoro RJ. 1995. Impinging jet injector atomization. See Yang & Anderson 1995, Chapter 8

Andreas EL, Pattison M, Belcher SE. 2001. Production rates of sea-spray droplets: Clarification and elaboration. *J. Phys. Res.* 106(C4):7157–61

Anguelova M, Barber RP. 1999. Spume drops produced by the wind tearing of wave crests. *J. Phys. Oceanogr.* 29:1156–65

Ashgriz N, Poo YL. 1990. Coalescence and separation in binary collisions of liquid drops. *J. Fluid Mech.* 221:183–204

Bauer-Agricola G. 1556. *De Re Metallica*. Basel: Froben

Bayvel L, Orzechowski Z. 1993. *Liquid Atomization*, ed. N Chigier. Washington, DC: Taylor & Francis

Bentley W. 1904. Studies of raindrops and raindrop phenomena. *Mon. Weather Rev.* 10:450–56

Blanchard D. 1966. *From Raindrops to Volcanoes*. New York: Dover

Born M. 1969. *Atomic Physics*. New York: Dover

Bremond N, Villermaux E. 2005. Bursting thin liquid films. *J. Fluid Mech.* 524:121–30

Bremond N, Villermaux E. 2006. Atomization by jet impact. *J. Fluid Mech.* 549:273–306

Bréchignac C, Cahuzac P, Carlier F, Colliex C, Leroux J, et al. 2002. Instability driven fragmentation of nanoscale fractal islands. *Phys. Rev. Lett.* 88(19):196103

Burton J, Waldrep R, Taborek P. 2005. Scaling and instabilities in bubble pinch-off. *Phys. Rev. Lett.* 94:184502

Bush JWM, Hasha AE. 2004. On the collision of laminar jets: Fluid chains and fishbones. *J. Fluid Mech.* 511:285–310

Chandrasekhar S. 1961. *Hydrodynamic and Hydromagnetic Stability*. New York: Dover

Chen Y-J, Steen PH. 1997. Dynamics of inviscid capillary breakup: collapse and pinchoff of a film bridge. *J. Fluid Mech.* 341:245–67

Chou WH, Faeth GM. 1998. Temporal properties of secondary drop breakup in the bag breakup regime. *Int. J. Multiphase Flow* 24:889–912

Clanet C, Villermaux E. 2002. Life of a smooth liquid sheet. *J. Fluid Mech.* 462:307–40

Clay PH. 1940. The mechanism of emulsion formation in turbulent flow, Part 1. *Proc. R. Acad. Sci. Amsterdam* 43:852–65

Cohen RD. 1990. Steady-state cluster size distribution in stirred suspensions. *J. Chem. Soc. Faraday Trans.* 86(12):2133–38

Cohen RD. 1991. Shattering of a liquid drop due to impact. *Proc. R. Soc. London Ser. A* 435:483–503

Coulaloglou C, Tavlarides L. 1977. Description of interaction processes in agitated liquid-liquid dispersions. *Chem. Eng. Sci.* 32:1289–97

Coulson JM, Richardson JF. 1968. *Chemical Engineering*. New York: Pergamon

Crapper GD, Dombrowski N, Jepson WP, Pyott GAD. 1973. A note on the growth of kelvin-helmholtz waves on thin liquid sheets. *J. Fluid Mech*. 57:671–72
Della Porta G, De Vittori C, Reverchon E. 2005. Supercritical assisted atomization: A novel technology for microparticles preparation of an asthma-controlling drug. *AAPS PharmSciTech* 6(3):E421–28
Derrida B, Godrèche C, Yekutieli I. 1991. Scale-invariant regimes in one-dimensional models of growing and coalescing droplets. *Phys. Rev. A* 44(10):6241–51
Dombrowski N, Hooper PC. 1963. A study of the sprays formed by impinging jets in laminar and turbulent flow. *J. Fluid Mech*. 18:392–400
Dombrowski N, Jonhs WR. 1963. The aerodynamics instability and disintegration of viscous liquid sheets. *Chem. Eng. Sci*. 18:203–14
Dombrowski N, Neale ND. 1974. Formation of streams of uniform drops from fan spray pressure nozzles. *J. Aerosol Sci*. 5:551–55
Eaton JK, Fessler JR. 1994. Preferential concentration of particles by turbulence. *Int. J. Multiph. Flows* 20:169–209
Eggers J. 1997. Nonlinear dynamics and breakup of free-surface flows. *Rev. Mod. Phys*. 69(3):865–929
Eggers J. 2002. Dynamics of liquid nanojets. *Phys. Rev. Lett*. 89(8):084502
Einsenklam P. 1964. On ligament formation from spinning disks and cups. *Chem. Eng. Sci*. 19:693–94
Elbaum M, Lipson S. 1994. How does a thin wetted film dry up? Phys. *Rev. Lett*. 72(22):3562–65
Englman R. 1991. Fragments of matter from maximum-entropy viewpoint. *J. Phys. Condens. Matter* 3:1019–53
Faeth G, Hsiang L-P, Wu P-K. 1995. Structure and breakup properties of sprays. *Int. J. Multiph. Flows* 21:99–127
Falkovich G, Fouxon A, Stepanov M. 2002. Acceleration of rain initiation by turbulence. *Nature* 419:151–54
Faragó Z, Chigier N. 1992. Morphological classification of disintegration of round liquid jets in a coaxial air stream. *At. Sprays* 2:137–53
Feller W. 1971. *An Introduction to Probability Theory and Its Applications*, Vol. 2. New York: Wiley
Fisher M. 1967. The theory of condensation and the critical point. *Physics* 3:255–83
Frankel I, Weihs D. 1985. Stability of a capillary jet with linearly increasing axial velocity (with application to shaped charge). *J. Fluid Mech*. 155:289–307
Fraser RP, Dombrowski N, Routley JH. 1963. Thin filming of liquids by spinning cups. *Chem. Eng. Sci*. 18:323–37
Fraser RP, Eisenklam P, Dombrowski N, Hasson D. 1962. Drop formation from rapidly moving liquid sheet. *AIChE J*. 8:672–80
Friedlander SK, Wang C. 1966. The self-preserving particle size distribution for coagulation by brownian motion. *J. Colloid Interface Sci*. 22:126–32
Frisch U, Sornette D. 1997. Extreme deviations and applications. *J. Phys. I* 7:1155–71
Gladden J, Handzy N, Belmonte A, Villermaux E. 2005. Dynamic buckling and fragmentation in brittle rods. *Phys. Rev. Lett*. 94:035503
Gordillo J, Sevilla A, Rodriguez-Rodriguez J, Martinez-Bazant C. 2005. Axisymmetric bubble pinch-off at high Reynolds numbers. *Phys. Rev. Lett*. 95:194501

Gorokhovski MA, Saveliev VL. 2003. Analyses of Kolmogorov's model of breakup and its application into Lagrangian computation of liquid sprays under air-blast atomization. *Phys. Fluids* 15(1):184–92
Grady DE, Kipp ME. 1985. Geometric statistics and dynamic fragmentation. *J. Appl. Phys.* 58(3):1210–22
Hagerty WW, Shea JF. 1955. A study of the stability of plane fluid sheets. *J. Appl. Mech.* 22:509–14
Hanson AR, Domich EG, Adams HS. 1963. Shock tube investigation of the break-up of drops by air blasts. *Phys. Fluids* 6(8):1070–80
Heidmann MF, Priem RJ, Humphrey JC. 1957. A study of sprays formed by two impacting jets. *NACA Tech. Note 3835*
Heywood H. 1933. Characteristics of pulverized fuels. *J. Inst. Fuel* 6:241–48
Hinze JO. 1949. Fundamentals of the hydrodynamic mechanism of splitting in dispersion processes. *AIChE J.* 1(3):289–95
Hinze JO, Milborn H. 1955. Atomization of liquid by means of a rotating cup. *Trans. ASME: J. Appl. Mech.* 17:145–53
Hoyt JW, Taylor J. 1977. Waves on water jets. *J. Fluid Mech.* 83:119–27
Huang JCP. 1970. The break-up of axisymmetric liquid sheets. *J. Fluid Mech.* 43:305–19
James AJ, Vukasinovic B, Smith MK, Glezer A. 2003. Vibration-induced drop atomization and bursting. *J. Fluid Mech.* 476:1–28
Kapur J. 1989. *Maximum Entropy Models in Science and Engineering*. New York: Wiley
Kim I, Sirignano WA. 2000. Three-dimensional wave distortion and disintegration of thin planar liquid sheets. *J. Fluid Mech.* 410:147–83
Kolmogorov AN. 1941. On the lognormal distribution of the fragment sizes under grinding. *Dokl. Akad. Nauk SSSR* 31(2):99–101
Kolmogorov AN. 1949. On the breakage of drops in a turbulent flow. *Dokl. Akad. Nauk SSSR* 66(5):825–28
Kombayasi M, Gonda T, Isono K. 1964. Lifetime of water drops before breaking and size distribution of fragment droplets. *J. Meteorol. Soc. Jpn.* 42(5):330–40
Konno M, Aoki M, Saito S. 1983. Scale effect on breakup process in liquid-liquid agitated tanks. *J. Chem. Eng. Jpn.* 16(4):313–19
Krzeczkowski SA. 1980. Measurement of liquid droplet mechanism. *Int. J. Multiph. Flow* 6:227–39
Lane W. 1961. Shatter of drops in streams of air. *Ind. Eng. Chem.* 43(6):1312–17
Lavoisier AL. 1789. *Traîte Elémentaire de Chimie*. Paris: Cuchet
Laws JO, Parsons DA. 1943. The relation of raindrop-size to intensity. *Trans. Am. Geophys. Union* 24:452–60
Lefebvre AH. 1989. *Atomization and Sprays*. New York: Hemisphere
Lei X, Ackerson BJ, Tong P. 2001. Settling statistics of hard sphere particles. *Phys. Rev. Lett.* 86(15):3300–3
von Lenard P. 1904. Über regen. *Meteorol. Z.* 6:249 92–62
Lifshitz IM, Slyozov VV. 1961. The kinetics of precipitation from supersaturated solid solutions. *J. Phys. Chem. Solids* 19:35–50
Lin SP. 2003. *Breakup of Liquid Sheets and Jets*. Cambridge, UK: Cambridge Univ. Press

Loewen MR, O'Dor MA, Skafel MG. 1996. Bubbles entrained by mechanically generated breaking waves. *J. Geophys. Res.* 101(C9):452–60
Longuet-Higgins MS. 1992. The crushing of air cavities in a liquid. *Proc. R. Soc. London Ser. A* 439:611–26
Low TB, List R. 1982. Collision, coalescence and breakup of raindrops. Part 1. Experimentally established coalescence efficiencies and fragment size distributions in breakup. *J. Atmos. Sci.* 39:1591–1606
Lozano A, Garcia-Olivares A, Dopazo C. 1998. The instability growth leading to a liquid sheet break up. *Phys. Fluids* 10:2188–97
Mabile C, Leal-Calderon F, Bibette J, Schmitt V. 2003. Monodisperse fragmentation in emulsions: Mechanisms and kinetics. *Europhys. Lett.* 61(5):708–14
Mansour A, Chigier N. 1990. Disintegration of liquid sheets. *Phys. Fluids A* 2:706–19
Mariotte E. 1686. *Traité du Mouvement des Eaux et des Autres Corps Fluides*. Paris: E Michallet
Marmottant P, Villermaux E. 2004a. Fragmentation of stretched liquid ligaments. *Phys. Fluids* 16:2732–41. Erratum. 2006. *Phys. Fluids* 18:059901
Marmottant P, Villermaux E. 2004b. On spray formation. *J. Fluid Mech.* 498:73–112
Marschall J, Palmer WM. 1948. The distribution of raindrops with size. *J. Meteorol.* 5:165–66
Martinez-Bazan C, Montanes JL, Lasheras JC. 1999. On the breakup of an air bubble injected into a fully developed turbulent flow. Part 2. Size pdf of the resulting daughter bubbles. *J. Fluid Mech.* 401:183–207
Mason BJ. 1971. *The Physics of Clouds*. Oxford, UK: Clarendon
Massel S. 1996. *Ocean Surface Waves: Their Physics and Prediction*. Singapore: World Sci.
Mayer JE, Mayer MG. 1966. *Statistical Mechanics*. New York: Wiley
Mayer W, Tamura H. 1996. Propellant injection in a liquid oxygen/gaseous hydrogen rocket engine. *J. Propuls. Power* 12(6):1137–47
Monin AS, Yaglom AM. 1975. *Statistical Fluid Mechanics: Mechanics of Turbulence*, Vol. 2. Cambridge, MA: MIT Press
Moseler M, Landman U. 2000. Formation, stability, and breakup of nanojets. *Science* 289:1165–69
Mott NF. 1947. Fragmentation of shell cases. *Proc. R. Soc. London Ser. A* 189:300–8
Novikov EA, Dommermuth DG. 1997. Distribution of droplets in a turbulent spray. *Phys. Rev. E* 56(5):5479–82
Oddershede L, Dimon P, Bohr J. 1993. Self organized criticality in fragmenting. *Phys. Rev. Lett.* 71(19):3107–10
Oliveira M, McKinley G. 2005. Iterated stretching and multiple beads-on-a-string phenomena in dilute solutions of high extensible flexible polymers. *Phys. Fluids* 17:071704
Park J, Huh KY, Li X, Renksizbulut M. 2004. Experimental investigation on cellular breakup of a planar liquid sheet from an air-blast nozzle. *Phys. Fluids* 16:625–32
Pilch M, Erdman C. 1987. Use of breakup time data and velocity history data to predict the maximum size of stable fragments for acceleration-induced breakup of a liquid drop. *Int. J. Multiph. Flow* 13(6):741–57

Plateau J. 1873. *Statique Expérimentale et Théorique des Liquides Soumis aux Seules Forces Moléculaires*. Paris: Gautier-Villars
Pomeau Y, Villermaux E. 2006. Two hundred years of capillarity research. *Phys. Today* 3:39–44
Qian J, Law C. 1997. Regimes of coalescence and separation in droplet collision. *J. Fluid Mech*. 331:59–80
Ranger A, Nicholls J. 1969. Aerodynamic shattering of liquid drops. *AIAA J*. 7(2):285–90
Rayleigh L. 1879. On the instability of jets. *Proc. London Math. Soc*. 4:4–13
Rayleigh L. 1880a. On the resultant of a large number of vibrations of the same pitch and of arbitrary phase. *Philos. Mag.* 10:73–78
Rayleigh L. 1880b. On the stability, or instability of certain fluid motion. *Proc. London Math. Soc.* 11:57
Rayleigh L. 1891. Some applications of photography. *Nature* 44:249–54
Reiner G. 1992. Dewetting of thin polymer films. *Phys. Rev. Lett*. 68(1):75–78
Roberts JB, Spanos PD. 1999. *Random Vibrations and Statistical Linearization*. New York: Dover
Rosin P, Rammler E. 1933. The laws governing the fineness of powered coal. *J. Inst. Fuel* 7X:29–36
Ryan HM, Anderson WE, Pal S, Santoro RJ. 1995. Atomization characteristics of impinging liquid jets. *J. Propuls. Power* 11:135–45
Saffman PG, Turner J. 1956. On the collision of drops in a turbulent cloud. *J. Fluid Mech*. 1:16–30
Savart F. 1833a. Mémoire sur la constitution des veines liquides lancées par des orifices circulaires en mince paroi. *Ann. Chim.* 53:337–98
Savart F. 1833b. Mémoire sur le choc de deux veines liquides animées de mouvements directement opposés. *Ann. Chim.* 55:257–310
Savart F. 1833c. Mémoire sur le choc d'une veine liquide lancée sur un plan circulaire. *Ann. Chim.* 54:56–87
Savart F. 1833d. Suite du mé moire sur le choc d'une veine liquide lancé e sur un plan circulaire. *Ann. Chim.* 54:113–45
Schumann TEW. 1940. Theoretical aspects of the size distribution of fog particles. *Q. J. R. Meteorol. Soc*. 66:195–207
Seinfeld JH, Pandis SN. 1998. *Atmospheric Chemistry and Physics: From Air Pollution to Climate Change*. New York: Wiley
Shinnar R. 1961. On the behaviour of liquid dispersions in mixing vessels. *J. Fluid Mech*. 10:259–75
Simmons HC. 1977a. The correlation of drop-size distributions in fuel nozzle sprays. Part I. The drop-size/volume-fraction distribution. *J. Eng. Power* 7:309–14
Simmons HC. 1977b. The correlation of drop-size distributions in fuel nozzle sprays. Part II. The drop-size/number distribution. *J. Eng. Power* 7:315–19
Sovani S, Sojka P, Lefebvre A. 2000. Effervescent atomization. *Progr. Energy Combust. Sci*. 27:483–521
Squire HB. 1953. Investigation of the stability of a moving liquid film. *Br. J. Appl. Phys*. 4:167–69

Squires TM, Quake SR. 2005. Microfluidics: Fluid physics at the nanoliter scale. *Rev. Mod. Phys*. 77:977–1026
Srivastava R. 1971. Size distribution of raindrops generated by their breakup and coalescence. *J. Atmos. Sci*. 28:410–15
Stern SA, Weaver HA, Steffl AJ, Mutchler MJ, Merline WJ, et al. 2006. A giant impact origin for Pluto's small moons and satellite multiplicity in the Kuiper belt. *Nature* 439:946–48
Stockmayer WH. 1943. Theory of molecular size distribution and gel formation in branched-chain polymers. *J. Chem. Phys*. 11(2):45–55
Stone HA, Stroock AD, Adjari A. 2004. Engineering flows in small devices: Microfluidics towards a lab-on-a-chip. *Annu. Rev. Fluid Mech*. 36:381–411
Stow CD, Stainer RD. 1977. The physical products of a splashing water drop. *J. Meterol. Soc. Jpn*. 55(5):518–31
Sultan E, Boudaoud A. 2006. The statistics of crumpled paper. *Phys. Rev. Lett*. 96:136103
Taylor GI. 1959a. The dynamics of thin sheets of fluid. II. Waves on fluid sheets. *Proc. R. Soc. London* 253:296–312
Taylor GI. 1959b. The dynamics of thin sheets of fluid. III. Disintegration of fluid sheets. *Proc. R. Soc. London* 253:313–21
Taylor GI. 1960. Formation of thin flat sheets of water. *Proc. R. Soc. London* 259:1–17
Thoroddsen ST, Etoh TG, Takehara K. 2006. Crown breakup by Marangoni instability. *J. Fluid Mech*. 557:63–72
Thoroddsen ST, Takehara K. 2000. The coalescence cascade of a drop. *Phys. Fluids* 12(6):1265–67
Trouton FT. 1906. On the coefficient of viscous traction and its relation to that of viscosity. *Proc. R. Soc. London* 77:426–40
Tucker C, Moldenaers P. 2002. Microstructural evolution in polymer blends. *Annu. Rev. Fluid Mech*. 34:177–210
Valentas K, Amundson NR. 1966. Breakage and coalescence in dispersed phase systems. *I&EC Fund.* 5(4):533–42
Villermaux E. 1998a. Mixing and spray formation in coaxial jets. *J. Propuls. Power* 14:807–17
Villermaux E. 1998b. On the role of viscosity in shear instabilities. *Phys. Fluids* 10:368–73
Villermaux E, Clanet C. 2002. Life of a flapping liquid sheet. *J. Fluid Mech*. 462:341–63
Villermaux E, Duplat J. 2003. Mixing as an aggregation process. *Phys. Rev. Lett*. 9(18):184501
Villermaux E, Marmottant P, Duplat J. 2004. Ligament-mediated spray formation. *Phys. Rev. Lett*. 92:074501
von Neumann J. 1952. Discussion. *Metal Interfaces*, pp. 108–10. Cleveland, OH: Am. Soc. Metals
von Smoluchowski M. 1917. Versuch einer mathematischen theorie der koagulationskinetik kolloider lösungen. *Z. Phys. Chem*. 92:129–68
Weber C. 1931. Zum zerfall eines flssigkeitsstrahles. *Z. Angew. Math. Mech*. 112:136–54

Wittel F, Kun F, Hermann H, Kroplin B. 2004. Fragmentation of shells. *Phys. Rev. Lett*. 93(3):035504

Worthington AM. 1908. *A Study of Splashes*. Longmans, Green

Wu J. 1981. Bubble populations and spectra in near-surface ocean: summary and review of field measurements. *J. Geophys. Res.* 86(C1):457–63

Wu P-K, Faeth G. 1995. Onset and end drop formation along the surface of turbulent jets in still gases. *Phys. Fluid* 7(11):2915–17

Yang V, Anderson W, eds. 1995. *Liquid Rocket Engine Combustion Instability*, Vol. 169. Washington, DC: AIAA

Yarin AL. 2006. Drop impact dynamics: Splashing, spreading, receding, bouncing. . . . *Annu. Rev. Fluid Mech*. 38:159–92

York JL, Stubbs HE, Tek MR. 1953. The mechanism of disintegration of liquid sheets. *Trans. ASME* 75:1279–86

Annual Review of
Fluid Mechanics

Volume 39, 2007

Contents

Indexes

Errata

An online log of corrections to *Annual Review of Fluid Mechanics* chapters (1997 to the present) may be found at http://fluid.annualreviews.org/errata.shtml